

ISSN: 0095-8972 (Print) 1029-0389 (Online) Journal homepage: <http://www.tandfonline.com/loi/gcoo20>


A disparate 3-D silver(I) coordination polymer of pyridine-3,5-dicarboxylate and pyrimidine with strong intermetallic interactions: X-ray crystallography, photoluminescence and antimicrobial activity

Sevim Hamamci Alisir, Serkan Demir, Bahtiyar Sariboga & Orhan Buyukgungor


To cite this article: Sevim Hamamci Alisir, Serkan Demir, Bahtiyar Sariboga & Orhan Buyukgungor (2015) A disparate 3-D silver(I) coordination polymer of pyridine-3,5-dicarboxylate and pyrimidine with strong intermetallic interactions: X-ray crystallography, photoluminescence and antimicrobial activity, *Journal of Coordination Chemistry*, 68:1, 155-168, DOI: [10.1080/00958972.2014.978307](https://doi.org/10.1080/00958972.2014.978307)


To link to this article: <http://dx.doi.org/10.1080/00958972.2014.978307>

 View supplementary material 



 Published online: 14 Nov 2014.

 Submit your article to this journal 

 Article views: 110

 View related articles 

 View Crossmark data 

 Citing articles: 4 View citing articles 

A disparate 3-D silver(I) coordination polymer of pyridine-3,5-dicarboxylate and pyrimidine with strong intermetallic interactions: X-ray crystallography, photoluminescence and antimicrobial activity

SEVIM HAMAMCI ALISIR*[†], SERKAN DEMIR[‡], BAHTIYAR SARIBOGA[§] and ORHAN BUYUKGUNGOR[¶]

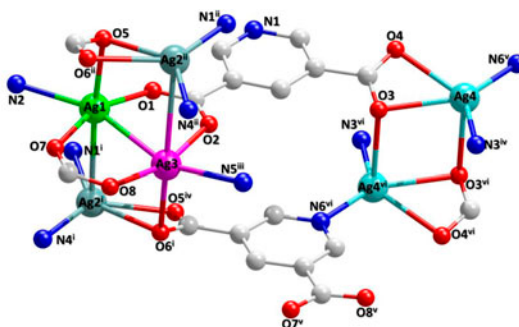
[†]Faculty of Engineering, Department of Materials Science and Engineering, Ondokuz Mayıs University, Samsun, Turkey

[‡]Faculty of Arts and Sciences, Department of Chemistry, Ondokuz Mayıs University, Samsun, Turkey

[§]School of Health, Sinop University, Sinop, Turkey

[¶]Faculty of Arts and Sciences, Department of Physics, Ondokuz Mayıs University, Samsun, Turkey

(Received 28 February 2014; accepted 10 September 2014)



A polymeric silver(I) complex $[Ag_4(\mu\text{-pydc})_2(\mu\text{-pm})_2]_n$ (**1**) consisting four coordinatively different silver(I) centers with excellent complementary assembly of pyridine-3,5-dicarboxylate (*pydc*) and pyrimidine (*pm*) ligands. 3D crystal structure of **1** has been determined by X-ray single crystal analysis and it has been identified that existence of intriguing close intermetallic interactions in addition to the presence of differently coordinating two *pydc* ligands. Strong solid-state fluorescence property and, effective antimicrobial behaviour of **1** has been also demonstrated.

A polymeric silver(I) complex, $[Ag_4(\mu\text{-pydc})_2(\mu\text{-pm})_2]_n$ (**1**) (*pydc* = pyridine-3,5-dicarboxylate and *pm* = pyrimidine), has been synthesized and characterized by elemental analysis, IR spectroscopy, thermal analysis, and single-crystal X-ray diffraction. X-ray crystallographic data of **1** revealed that *pydc* exhibits two different coordination modes that play a key role in the construction of the 3-D crystal network including Ag–carboxylate clusters in which close Ag–Ag distances exist. The magnitudes of close Ag–Ag interactions in second-order energy (E^2) have been revealed by natural bond orbital analysis performed with single point energy calculation using the experimental geometry of **1**. Furthermore, the luminescent properties of **1** show strong fluorescence with two emission maxima in

*Corresponding author. Email: sevimh@omu.edu.tr

the visible region. Also, **1** has antifungal activity on *Candida albicans* (MIC value, 4 $\mu\text{g mL}^{-1}$) and good antibacterial activity on micro-organisms (MIC value, 64–256 $\mu\text{g mL}^{-1}$).

Keywords: Silver(I) complex; Pyridine-3,5-dicarboxylate; Coordination polymer; Photoluminescent properties; Antimicrobial properties

1. Introduction

Rapid expansion of crystal engineering of higher dimensional coordination polymers arise from unrivaled structural diversity [1–3] and potential applications as functional materials [4–9]. The design and synthesis of organic–inorganic hybrid materials with unique structures and functions are difficult. In principle, desired structural features and/or physico-chemical properties depend on the nature of the organic ligands and metal ions rather than reaction conditions [10]. Therefore, exploration of novel entangled coordination polymers have remained a long-term challenge, and comprehensive research is necessary to enrich and develop this field.

Ag(I)-containing coordination complexes have attracted attention due to unpredictable coordination preferences of the metal center and the formation of close Ag(I)⋯Ag(I) interaction which is directly associated with photoluminescent properties and use as potential antibacterial agents. In the design and synthesis of coordination polymers, various bridging and chelating ligands such as pyridinedicarboxylic acids (2,3-, 2,5-, 2,6-, 3,4-, and 3,5-*pydc*) have been used. Numerous reports of coordination polymers constructed by (2,3-, 2,5-, 2,6-, and 3,4-*pydc*) have been reported [11–16], but only a few reports of coordination polymers where 3,5-*pydc* was used as chelator or bridging ligand and most focused on those with Cu(II), Ni(II), Pd(II), and Eu(III) [17–20]. A few silver(I) complexes have been synthesized with 3,5-*pydc*, $[\text{Ag}_5(\text{pydc})_2(\text{OH})]$, $[\text{Ag}_5(\text{pydc})_2(\text{CN})]_n$, $\{[\text{Ag}_4(\text{pydc})_2]\text{CH}_3\text{CN}\}_n$, and $[\text{Ag}_2(\text{bpy})_2(\text{H}_2\text{O})(\text{pydc})\cdot 3\text{H}_2\text{O}]$ [21–23]. However, the coordination features of this ligand in which the silver(I) complexes have different auxiliary ligands have not been widely investigated.

Considering the above-mentioned points, we have synthesized a new 3-D silver(I)-pyridine-3,5-dicarboxylate coordination polymer, $[\text{Ag}_4(\mu\text{-pydc})_2(\mu\text{-pm})_2]_n$ (**1**), which is a mixed-ligand silver(I) complex {*pydc* = pyridine-3,5-dicarboxylate, *pm* = pyrimidine}, investigated the luminescent properties and antimicrobial activity of **1**.

2. Experimental

2.1. Materials

All reagents for the synthesis were supplied commercially and used without purification. IR spectra were recorded on a Perkin Elmer Spectrum Two FT-IR spectrophotometer from 4000 to 600 cm^{-1} . Elemental analyses (C, H, and N) were determined on a LECO CHNS-932 elemental analyser. Thermal analysis curves (TG, DTA, DTG) were recorded simultaneously on a Shimadzu DTG-60 thermal analyzer in static air at 10 $^\circ\text{C min}^{-1}$ heating rate from 20 to 600 $^\circ\text{C}$ using platinum crucibles. The fluorescence (excitation and emission) spectra in the solid state were recorded with a Perkin Elmer LS-55 spectrophotometer.

2.2. Synthesis of **1**

An aqueous solution (5 cm³) of AgNO₃ (0.17 g, 1 mM) was added to H₂pydc (0.17 g, 1 mM) dissolved in water (10 cm³) by adding NaOH solution and the pH was adjusted to 7. Upon addition of a methanolic solution (5 cm³) of pm (0.10 g, 1 mM) to the stirring suspension of the white precipitate, a bright clear solution was obtained. Well formed pale yellow crystals of **1** in X-ray quality were obtained within several days with slow evaporation of the solvent from the solution at room temperature in the dark. Yield: 76% based on Ag, dp: 190 °C, FT-IR (KBr; cm⁻¹, s: strong; m: middle; w: weak): 3065(w), 1603(s), 1584(s), 1557(s), 1408(s), 1395(m), 1362(s), 1353(s), 1227(m), 1118(w), 1033(w), 922(w), 819(w), 768(m), 729(m), 685(s). Anal. data (%) for [C₂₂H₁₄N₆O₈Ag₄]: Found: C, 28.07; H, 1.84; N, 8.64; Calcd: C, 28.66; H, 1.53; N, 9.12.

2.3. X-ray crystallography

Data collection for **1** was performed on a STOE IPDS II image plate detector using Mo K α radiation ($\lambda = 0.71019$ Å) at 293 K. The structure was solved by direct methods using SHELXS-97 and refined by full-matrix least-squares procedure on F^2 (SHELXL-97) [24]. Solvent in **1** was performed by using the program SQUEEZE incorporated in PLATON [25, 26]. All hydrogens in **1** were included in calculated positions and refined with fixed thermal parameters riding on their parent atoms. The details of data collection, refinement, and crystallographic data are summarized in table 1.

Table 1. Crystal data and structure refinement parameters for [Ag₄(μ -pydc)₂(μ -pm)₂]_n (**1**).

Empirical formula	C ₂₂ H ₁₄ N ₆ O ₈ Ag ₄
Formula weight	921.87
Temperature (K)	293
Wavelength (Å)	0.71073
Crystal system	Monoclinic
Space group	C2/c
<i>Unit cell dimensions</i>	
<i>a</i> , <i>b</i> , <i>c</i> (Å)	26.8616(16), 14.8443(10), 12.5502(8)
α , β , γ (°)	90.00, 107.393(5), 90.00
<i>V</i> (Å ³)	4775.5(5)
<i>Z</i>	8
<i>D</i> _{calcd} (g cm ⁻³)	2.564
μ (mm ⁻¹)	3.297
<i>F</i> (0 0 0)	3520
θ Range (°)	2.14 to 27.38
Index range	-28 $\leq h \leq$ +33, -18 $\leq k \leq$ +18, -15 $\leq l \leq$ +15
Independent reflections	4965
Reflections observed ($>2\sigma$)	3417
Data/parameters	3417/361
Absorption correction	Integration
<i>T</i> _{min} , <i>T</i> _{max}	0.3694, 0.7282
Final <i>R</i> indices [<i>I</i> $> 2\sigma(I)$]	<i>R</i> ₁ = 0.0393, <i>wR</i> ₁ = 0.0936
Goodness-of-fit on F^2	1.018
$\Delta\rho_{\max}$ (e Å ⁻³)	1.067
$\Delta\rho_{\min}$ (e Å ⁻³)	-1.503

2.4. Antimicrobial activity tests

The potential antibacterial effects of **1** were investigated by micro dilution against five gram-positive bacteria *Bacillus cereus* (ATCC 7064), *Enterococcus faecalis* (ATCC 15753), *Listeria monocytogenes* (ATCC 19114), *Streptococcus pneumoniae* (ATCC 29212), *Staphylococcus aureus* (ATCC 6538), and *Methicillin Resistant Staphylococcus aureus* MRSA (ATCC 43300), three gram-negative bacteria *Salmonella typhi* (CCM 5445), *Escherichia coli* (ATCC35218), *Pseudomonas aureginosa* (ATCC27853), and a yeast *Candida albicans* (ATCC 10231). The complex was dissolved in water/acetonitrile (4/3) to a final concentration of 4096 $\mu\text{g mL}^{-1}$ and then sterilized by filtration using 0.20 μm Millipore. Negative controls were prepared by using water/acetonitrile (4/3). Vancomycin and ciprofloxacin were used as positive reference standards. The bacteria were incubated in Muller Hinton Broth (MHB, Oxoid) at 37 °C for 24 h. The antibacterial activity assays of the compounds were performed according to the clinical and laboratory standards institute protocols [27]. The antifungal activities of all compounds were evaluated according to the National Committee for Clinical Laboratory Standards [28]. The yeast was incubated in RPMI-1640 medium (Biological Industries) at 35 °C for 48 h. Antifungal activity of the reference drug, Amphotericin-B (Sigma), was also assessed under similar conditions. The minimum inhibitor concentration (MIC, $\mu\text{g mL}^{-1}$) value was determined as the lowest concentration at which the growth of bacteria was not observed. All experiments were performed in duplicate and confirmed by three separate experiments.

2.5. Computational details

Single point energy (SPE) calculation was performed using Gaussian 09W suite running under windows [29] and hybrid DFT/B3LYP functional was used applying LANL2DZ ECP basis set for all atoms within tolerable computational expense.

3. Results and discussion

3.1. Thermal analysis

Thermal decomposition behavior of $[\text{Ag}_4(\mu\text{-pydc})_2(\mu\text{-pm})_2]_n$ was followed to 600 °C in static air. The TG, DTA, and DTG curves are illustrated in figure 1. The compound does not melt and is stable to 190 °C at which it begins to decompose, displaying two mass loss steps. The first between 190 and 234 °C corresponds to endothermic removal of *pm* (DTA max 222 °C). The experimental mass loss of 17.99% for this stage agrees with the calculated mass loss of 17.35%. Continuous mass loss to 383 °C is observed at the subsequent stage, related to release of *pydc* with a mass loss of 35.40% (Calcd 35.79%) and related DTA curve displays a sharp exothermic peak at 356 °C. The remaining mass of 46.61% is related to metallic silver, in agreement with calculated value of 46.86%.

3.2. Crystal structure of $[\text{Ag}_4(\mu\text{-pydc})_2(\mu\text{-pm})_2]_n$

X-ray crystallographic analysis shows that the complex crystallizes in the monoclinic space group *C2/c* and has a 3-D polymeric network with bridging through *pydc* and *pm* ligands.

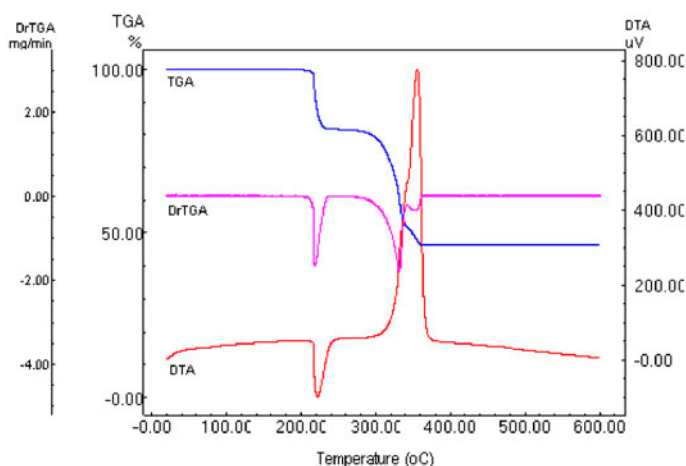


Figure 1. The TG, DTA, and DTG curves of **1**.

All carboxylates of H_2pydc in **1** are deprotonated, in agreement with IR data in which no strong absorption at 1700 cm^{-1} is observed for $-\text{COOH}$. The spectrum of **1** also shows characteristic bands of carboxylate between 1584 , 1557 , and 1408 cm^{-1} for antisymmetric stretch and at 1395 , 1362 , and 1353 cm^{-1} for symmetric stretch as multiple-peaks (figure S1, see online supplemental material at <http://dx.doi.org/10.1080/00958972.2014.978307>). The difference between the asymmetric and symmetric carboxylate stretch ($\Delta\nu = \nu_{\text{as}}(-\text{COO}^-) - \nu_{\text{s}}(\text{COO}^-)$) is used to correlate the infrared spectra of metal carboxylate structures. The value of $\Delta\nu$ is reported as ~ 270 , ~ 165 , and $\sim 60\text{ cm}^{-1}$ for the unidentate, bridging, and chelating carboxylate groups, respectively [30]. The ($\Delta\nu = \nu_{\text{as}} - \nu_{\text{s}}$) values are 195 , 189 , and 55 cm^{-1} in **1**, suggesting bridging and chelating carboxylates of $pydc$.

In the complex, the $pydc$ ligands have two different bridging modes, each denoted with superscripts, $pydc^{(a)}$ and $pydc^{(b)}$, to distinguish from each other as depicted in scheme 1. $pydc^{(a)}$ displays a $\mu_5-\eta^5$ bridging mode while $pydc^{(b)}$ has $\mu_6-\eta^5$ mode via all donors.

In **1**, there are four crystallographically independent silvers, each with different coordination (figure 2). Ag1 is four coordinate in a significantly distorted tetrahedral geometry with three oxygens (O1 from the $pydc^{(a)}$, O5 and O7 from the $pydc^{(b)}$) from two different $pydc$ ligands and N2 from pm coordinated to Ag1 (table 2).

Ag2 is bound to O5ⁱⁱ and O6 of the chelating carboxylate of $pydc^{(b)}$, N1 of $pydc^{(a)}$, and N4 of a second pm to construct a highly distorted tetrahedron with a AgN_2O_2 core. The discrimination parameter for AgN_2O_2 core ($(\tau_4 = [(360^\circ - (\alpha + \beta))/141^\circ])$, where α and β are the largest angles around the metal center) is 0.5865 and indicates substantial deviation from ideal tetrahedral geometry [31]. Ag3 is coordinated by one N5 of the second pm , O2 from the first (bridging) carboxylate of $pydc^{(a)}$, O6ⁱ from the second carboxylate of $pydc^{(b)}$, and O8 from the first carboxylate of $pydc^{(b)}$. $\text{Ag1}\cdots\text{Ag3}$, $\text{Ag1}\cdots\text{Ag2}^i$, and $\text{Ag3}\cdots\text{Ag2}^{ii}$ distances ($2.914(7)$, $3.195(8)$, and $3.367(8)\text{ \AA}$) are significantly shorter than the sum of van der Waals radii for two silvers (3.44 \AA), indicating weak interactions between adjacent Ag(I) ions, which lead to a $[\text{Ag}_4(\text{COO})_4\text{N}_6]$ cluster. If coexisting strong argentophilic $\text{Ag1}\cdots\text{Ag3}$ and $\text{Ag1}\cdots\text{Ag2}^i$ interactions (figure 3) are considered as coordinative, the coordination around Ag1 is a significantly distorted octahedral geometry.

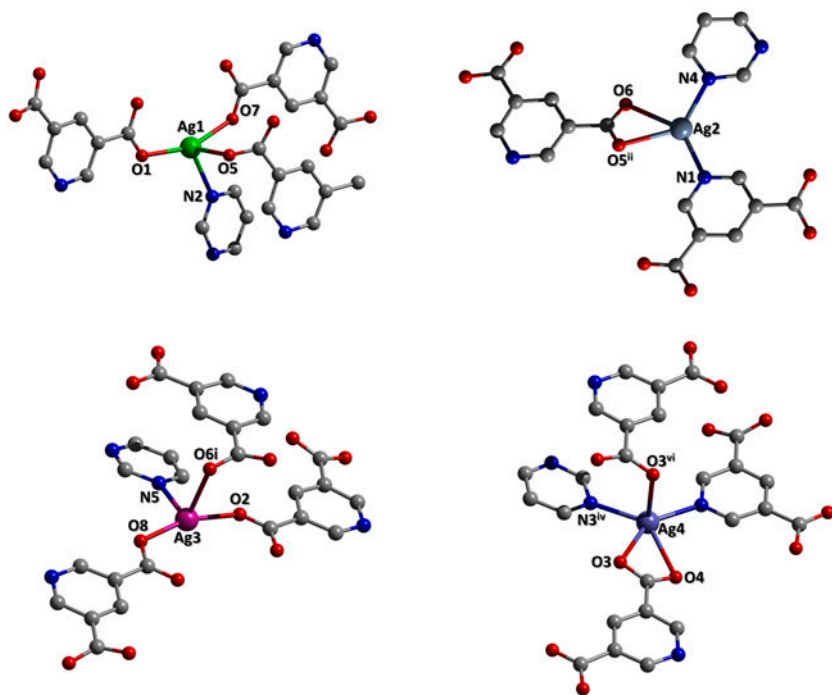


Figure 2. View of the coordination geometry of Ag(I) in $[\text{Ag}_4(\mu\text{-pydc})_2(\mu\text{-pm})_2]_n$.

Similar to the aforementioned argentophilic interactions, when close $\text{Ag1}\cdots\text{Ag2}^i$ and $\text{Ag3}\cdots\text{Ag2}^{ii}$ interactions are taken in account, the geometries both around Ag2 and Ag3 centers can be described as square-pyramidal with small deviations (the discrimination parameters (τ) for Ag2 and Ag3 were calculated as 0.1557 and 0.095, respectively). Ag4, the only center that is not incorporated into argentophilic interactions, is surrounded by O3 and O4 from second carboxylate of *pydc*^(a), symmetry related O3^{vi} from the same unit, N6^v from *pydc*^(b), and N3^{iv} from the first *pm*, and hence the five-coordinate Ag4 center in **1** has distorted square-pyramidal geometry ($\tau = 0.1033$).

The $[\text{Ag}_4(\text{COO})_4]$ core in **1** resembles a paddle-wheel cage structure with combinations of two syn–syn O1–C–O2 and O7–C–O8 bridges, two mono-atomic COO bridges through O5 and O6ⁱ, and close $\text{Ag1}\cdots\text{Ag2}^i$ and $\text{Ag3}\cdots\text{Ag2}^{ii}$ interactions as seen in figure 3. $[\text{Ag}_4(\text{COO})_4]$ cores are linked through carboxylate groups, leading to a 1-D chain (figure 4).

In the ac plane, **1** forms a 2-D coordination slab substructure which is constructed primarily from the junction of $[\text{Ag}_4(\text{COO})_4\text{N}_6]$ clusters through two syn-anti O5–C–O6ⁱⁱ and O5^{iv}–C–O6ⁱ bridges. $[\text{Ag}_4(\text{COO})_4\text{N}_6]$ clusters are adjoined cross-sectionally and sharing the same symmetrically equivalent Ag2 ions via monoatomic O5^{iv} and O6ⁱⁱ bridges each belonging also to O5^{iv}–C–O6ⁱ and O5–C–O6ⁱⁱ groups, respectively, as deduced from figures 3 and 5. Thus, O5^{iv}–C–O6ⁱ and O5–C–O6ⁱⁱ groups simultaneously exhibit both syn-anti and monoatomic bridging modes. $[\text{Ag}_2(\text{COO})_2]$ cores are also cross-oriented and linked to $[\text{Ag}_4(\text{COO})_4]$ cores with oppositely directed *pydc* ligands in 2-D construction.

The 2-D polymeric framework is further extended to a 3-D network with coordination of *pm* and *pydc* linkers depicted in figure 6.

Table 2. Selected bond distances (Å), angles (°), and hydrogen bonding geometries for **1**.

<i>Bond lengths (Å)</i>				
Ag1–O1	2.201(4)	Ag3–O2	2.238(4)	
Ag1–O5	2.588(5)	Ag3–O8	2.205(4)	
Ag1–O7	2.252(4)	Ag3–O6 ⁱ	2.257(5)	
Ag1–N2	2.436(5)	Ag3–N5 ⁱⁱⁱ	2.490(5)	
Ag2–N1	2.228(5)	Ag4–O3	2.468(5)	
Ag2–N4	2.264(5)	Ag4–O4	2.569(5)	
Ag2–O5 ⁱⁱ	2.460(5)	Ag4–N3 ^{iv}	2.313(5)	
Ag2–O6 ⁱⁱ	2.579(5)	Ag4–N6 ^v	2.253(5)	
Ag1–Ag2 ⁱ	3.195(8)	Ag4–O3 ^{vi}	2.704(5)	
Ag1–Ag3	2.914(7)	Ag3–Ag2 ⁱⁱ	3.367(8)	
Ag4–C16 ^v	3.151(6)	Ag4–C8 ^{iv}	3.252(6)	
Ag4–C9 ^{iv}	3.165(6)	Ag3–C13 ⁱⁱⁱ	3.278(6)	
Ag4–C20 ^v	3.173(6)			
<i>Bond angles (°)</i>				
O1–Ag1–O7	157.88(16)	O8–Ag3–O2	163.03(16)	
O1–Ag1–N2	114.00(17)	O8–Ag3–N5 ⁱⁱⁱ	106.23(17)	
O1–Ag1–O5	98.90(16)	O8–Ag3–Ag1	87.59(12)	
O1–Ag1–Ag3	84.32(12)	O8–Ag3–O6 ⁱ	100.27(16)	
O1–Ag1–Ag2 ^{vi}	81.78(12)	O2–Ag3–N5 ⁱⁱⁱ	86.24(17)	
O7–Ag1–N2	85.93(17)	O2–Ag3–Ag1	77.15(12)	
O7–Ag1–O5	88.42(16)	O2–Ag3–O6 ⁱ	88.01(17)	
O7–Ag1–Ag2 ^{vi}	88.52(12)	N5 ⁱⁱⁱ –Ag3–Ag1	157.34(12)	
N2–Ag1–O5	94.62(15)	N5 ⁱⁱⁱ –Ag3–O6 ⁱ	101.89(15)	
N2–Ag1–Ag3	158.74(13)	N6 ^v –Ag4–N3 ^{iv}	130.85(16)	
O5–Ag1–Ag3	92.92(10)	N6 ^v –Ag4–O3	142.17(16)	
N1–Ag2–N4	129.05(16)	N6 ^v –Ag4–O4	91.76(16)	
N1–Ag2–O5 ⁱⁱ	96.17(17)	N6 ^v –Ag4–O3 ^{vi}	91.25(16)	
N1–Ag2–O6 ⁱⁱ	143.32(16)	N3 ^{iv} –Ag4–O3	86.93(16)	
N1–Ag2–Ag ^{vi}	83.51(12)	N3 ^{iv} –Ag4–O4	135.99(15)	
N4–Ag2–O5 ⁱⁱ	133.98(17)	N3 ^{iv} –Ag4–O3 ^{vi}	91.04(16)	
N4–Ag2–O6 ⁱⁱ	86.34(16)	O3–Ag4–O4	52.10(15)	
N4–Ag2–Ag ^{vi}	92.00(12)	O3–Ag4–O3 ^{vi}	85.29(15)	
O5 ⁱⁱ –Ag2–O6 ⁱⁱ	52.07(16)	O4–Ag4–O3 ^{vi}	99.60(14)	
D–H⋯A	D–H (Å)	H⋯A (Å)	D⋯A (Å)	D–H⋯A (°)
C9–H9⋯O3	0.93	2.38	3.106(8)	135
C13–H13⋯O2	0.93	2.36	3.072(7)	133
C14–H14⋯O4	0.93	2.49	3.185(7)	132
C15–H15⋯O6	0.93	2.47	3.146(7)	130

Note: Symmetry operations: (i) $x, -y, -1/2 + z$; (ii) $-x, y, 1/2 - z$; (iii) $1/2 + x, -1/2 - y, 1/2 + z$; (iv) $x, -1 + y, z$; (v) $-x, -1 + y, 1/2 - z$; (vi) $-x, -1 - y, -z$.

A few coordination polymers constructed from silver and 3,5-pydc, $[\text{Ag}_5(\text{pydc})_2(\text{OH})]$ [21] $[\text{Ag}_5(\text{pydc})_2(\text{CN})]_n$, $\{[\text{Ag}_4(\text{pydc})_2]\text{CH}_3\text{CN}\}_n$ [22], and $[\text{Ag}_2(\text{bpy})_2(\text{H}_2\text{O})](\text{pydc}) \cdot 3\text{H}_2\text{O}$ [23] have been reported. The crystal structure of $[\text{Ag}_2(\text{bpy})_2(\text{H}_2\text{O})](\text{pydc}) \cdot 3\text{H}_2\text{O}$ is made up of cationic chains of $[\text{Ag}_2(\text{bpy})_2(\text{H}_2\text{O})]_{\infty}^{2n+}$, *pydc* ions and water molecules. The cationic charge of $[\text{Ag}_2(\text{bpy})_2(\text{H}_2\text{O})]_{\infty}^{2n+}$ chains is balanced by counter ions of deprotonated *pydc*. *Pydc* is a bridging ligand by using all donor sites in $[\text{Ag}_5(\text{pydc})_2(\text{OH})]_n$, $[\text{Ag}_5(\text{pydc})_2(\text{CN})]_n$, and $\{[\text{Ag}_4(\text{pydc})_2]\text{CH}_3\text{CN}\}_n$. However, as depicted in scheme 1, *pydc* is both bridging and chelating among the silver(I) centers in **1**, different from the literature. In **1**, the Ag–N_{pydc} bond distance of 2.228(5) Å is shorter than $[\text{Ag}_5(\text{pydc})_2(\text{OH})]_n$ (2.240(8) Å), $[\text{Ag}_5(\text{pydc})_2(\text{CN})]_n$ (2.240(7) Å), and $\{[\text{Ag}_4(\text{pydc})_2]\text{CH}_3\text{CN}\}_n$ (2.291(6) Å). The Ag–O_{pydc} distances from 2.201(4) to 2.704(5) Å are similar to those found in polymeric silver-*pydc* complexes $[\text{Ag}_5(\text{pydc})_2(\text{OH})]_n$, $[\text{Ag}_5(\text{pydc})_2(\text{CN})]_n$, and $\{[\text{Ag}_4(\text{pydc})_2]\text{CH}_3\text{CN}\}_n$.

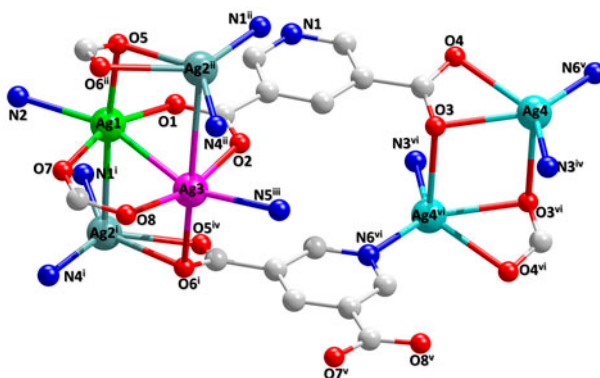


Figure 3. The structure of $[\text{Ag}_4(\text{COO})_4\text{N}_6]$ -cluster (left) and $[\text{Ag}_2(\text{COO})_2\text{N}_4]$ -cluster (right).

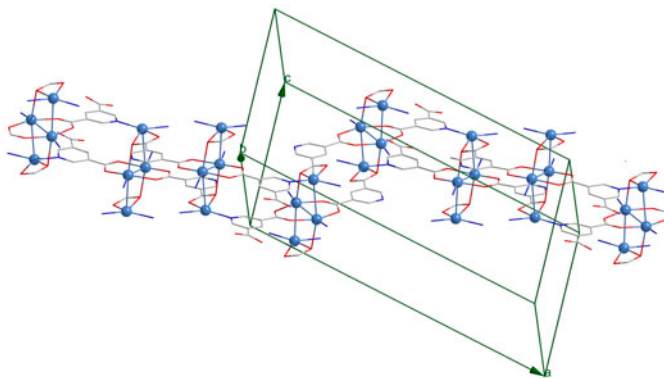


Figure 4. 1-D packing of $[\text{Ag}_4(\text{COO})_4\text{N}_6]$ -clusters in **1** along (a-c) diagonal through *pydc* bridges.

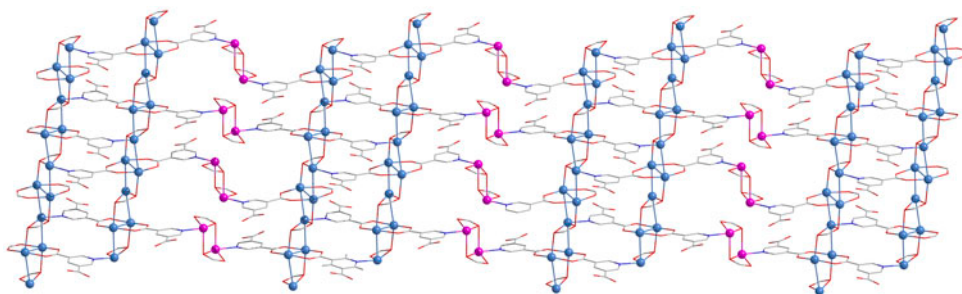


Figure 5. 2-D arrangement of $[\text{Ag}_4(\text{COO})_4\text{N}_6]$ - (blue) and $[\text{Ag}_2(\text{COO})_2\text{N}_4]$ - (pink) clusters along with a-c plane through only *pydc* linkers (see <http://dx.doi.org/10.1080/00958972.2014.978307> for color version).

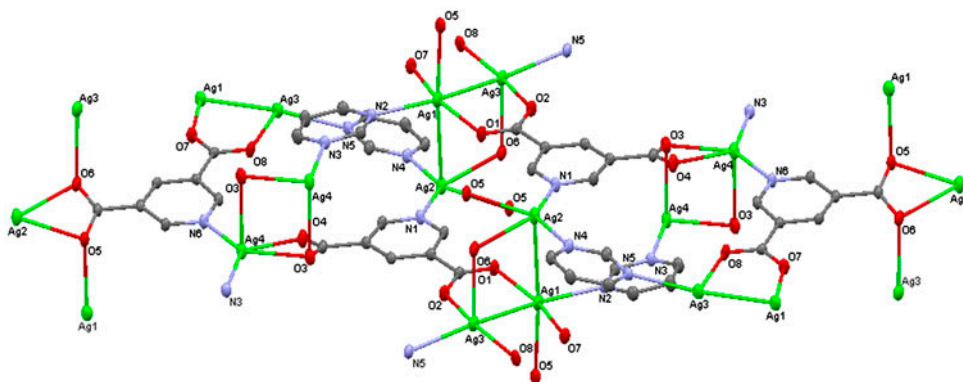


Figure 6. The 3-D metal–organic framework of **1** formed by bridging *pydc* and *pm* ligands.

The Ag...Ag separations in **1** are comparable to those found in $[\text{Ag}_5(\text{pydc})_2(\text{CN})]_n$ (3.0566 and 3.2316 Å) and $\{[\text{Ag}_4(\text{pydc})_2]\text{CH}_3\text{CN}\}_n$ (2.9166 and 3.2381 Å).

For two different *pm* ligands, the first connects Ag1 and Ag4 while the second connects Ag2 and Ag3 centers.

X-ray structure analysis reveals the presence of weak Ag...C (η^2) interactions between silver(I) ions and carbons of pyridine and pyrimidine rings. The Ag–C distances from 3.151 to 3.278 Å are noticeably shorter than the sum of van der Waals radii of Ag and carbon (3.42 Å). Selected interactions for **1** are given in table 2.

Some previous papers including polymeric silver(I) complexes of aromatic ligands reported similar Ag...C interactions with Ag–C distances of ca. 2.80–3.38 Å [32, 33]. Thus, these interactions in **1** may be considered as weak dihapto aromatic coordination of *pydc* and *pm* to the silver(I) ions. In addition to non-covalent $\text{Ag}4\cdots\text{C}_{\text{g}_{\text{pm}}}$ (3.891(2) Å), $\text{C}4\text{--H}4\cdots\text{C}_{\text{g}_{\text{pm}}}$ {(3.495 Å) (101.64°)} interactions, a large number of very weak intramolecular hydrogen bonds (table 2) and also weak $\pi\cdots\pi$ stacking interactions coexist in the structure. These interactions are significant for holding layers together in the solid state and reinforcing the 3-D framework.

3.3. SPE calculation

In order to emphasize the magnitude of close Ag(I)...Ag(I) interactions in energy, we have performed a simple SPE calculation on a fragment of the 3-D crystal network including $[\text{Ag}_4(\text{COO})_4]$ cluster in which the closest Ag–Ag distances exist and extracted the second-order energy (E^2) [34–37] data from natural bond orbital (NBO) analysis.

There is no doubt that the use of optimized geometries is only desirable in theoretical insight for all other subsequent computations to be meaningful. In particular, circumstances such as magnetochemical studies, the use of experimental geometries is requisite to obtain best results. For our structure containing strong and numerous close interactions, gas phase single molecule and solid state PBC optimizations do not give satisfactory results. Therefore, we have used the experimental geometry to quantitatively designate the close intermetallic interactions by NBO analysis. E^2 values of close Ag...Ag interactions are given in table 3. The values in the table are higher than the strongest van der Waals interactions and

Table 3. Second-order interaction energies among interacting Ag(I) ions.

Donor	Acceptor	Distance (Å)	E^2 (kJ M ⁻¹)
Ag1(LP*)	Ag3(RY*)	2.914	82.35
Ag1(LP*)	Ag2(RY*)	3.195	22.53
Ag2(LP*)	Ag3(LP*)	3.942	51.29
Ag2i(LP*)	Ag3(LP*)	3.367	75.36
Ag1(LP*)	Ag2i(LP*)	3.953	44.22

Note: LP*: antibonding lone pair valence orbital, RY*: Rydberg orbital.

are on the order of magnitude of a delta-bond. Second-order interactions take place between high energy lone pair and Rydberg orbitals. One may merely attribute this salient finding to facile delocalization of bulky 4d orbitals of Ag(I) ions even outside the valence orbitals that are effective between adjacent Ag(I) centers.

3.4. Photoluminescence analysis

Presence of coinage d¹⁰ metal or direct metal–metal interaction may be one of the important factors contributing to the photoluminescence, enhancing, shifting and quenching the luminescent emission of organic ligand by complexation [38]. Thus, the photoluminescence of **1** in the solid state at room temperature was examined.

As shown in figure 7, [Ag₄(μ-pydc)₂(μ-pm)₂]_n exhibits photoluminescence in the solid state at room temperature with two main emission peaks maximized at 540 and 583 nm

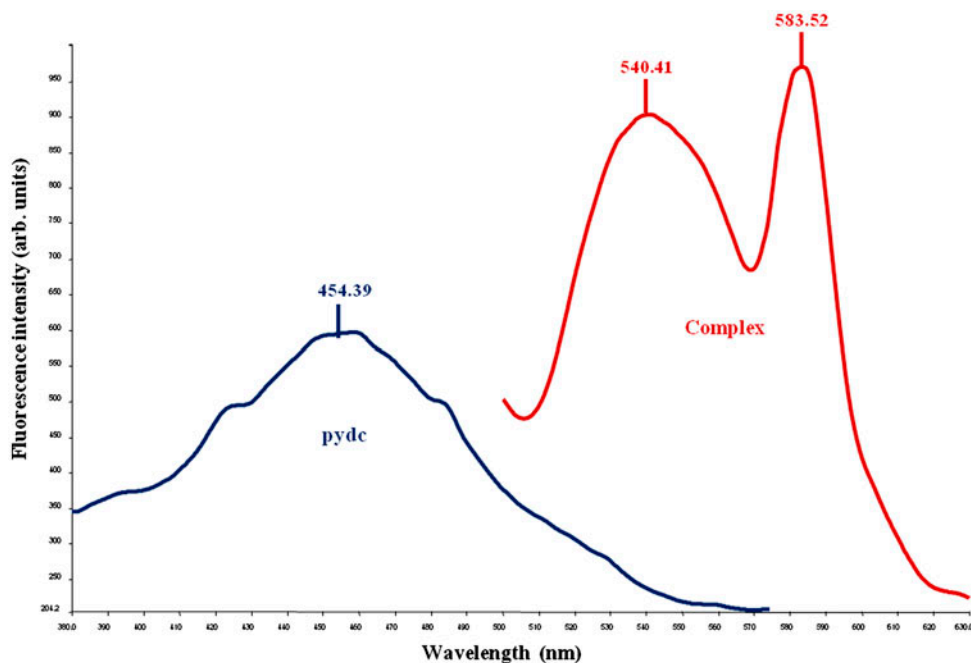
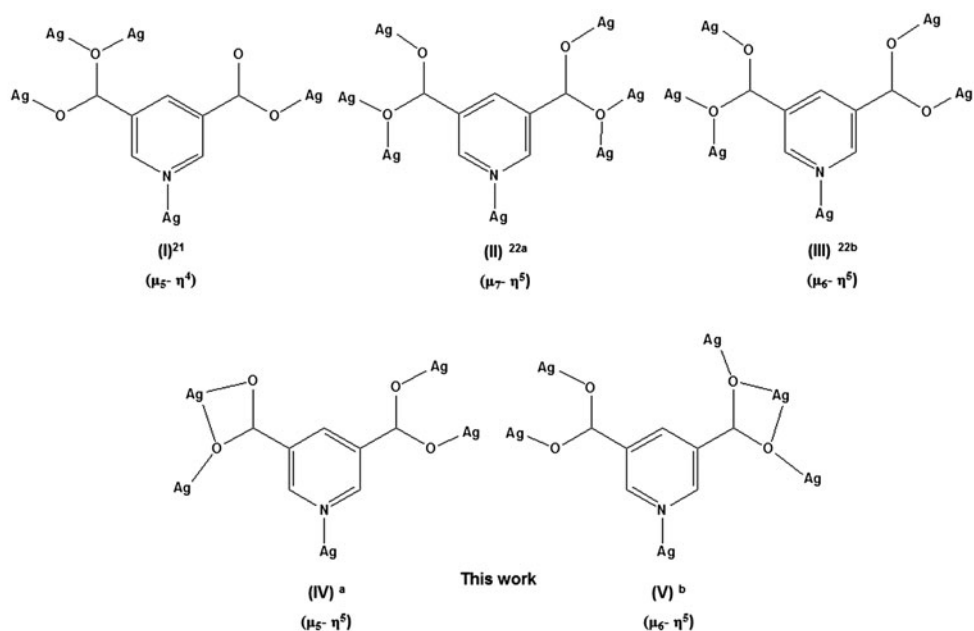


Figure 7. The solid state emission spectra of free H_2pydc and **1**.



Scheme 1. Various possible coordination modes of the pydc ligand with Ag [21, 22].

with excitation applied at 386 nm. In order to see the changes in emission spectrum upon complexation, we also measured the photoluminescence spectrum of free H_2pydc . Once excited at 310 nm, H_2pydc exhibits a broad emission with maximum at 454 nm. Compared to the photoluminescence spectrum of free H_2pydc , two distinct red-shifted emission bands were observed by complexation with metal. Furthermore, appreciable enhancement of luminescence in **1** is probably maintained by cluster-centered emission accompanied by ligand-to-metal charge transfer (LMCT) transitions mixed with metal-centered ones that are otherwise absent in free ligand (d-s/d-p). By comparison, the data obtained in this study demonstrated that **1** exhibits more intense photoluminescence than previously published silver(I) complexes of 3,5- $pydc$ [22]. This finding can be explained through the variations in 3-D architectures provoked by different intensities of supramolecular interactions (such as $\pi\cdots\pi$ interaction, $Ag\cdots Ag$ interaction). Such variations give rise to significant changes in HOMO-LUMO gap [22, 39, 40].

3.5. Antimicrobial activity

A summary of the *in vitro* antimicrobial activity experiments is presented in table 4. Complex **1** exhibits antibacterial activity against both gram-negative and gram-positive bacteria. The MIC value of **1** on the yeast *C. albicans* ($4\ \mu\text{g mL}^{-1}$) is quite significant. The complex shows the same MIC values ($128\ \mu\text{g mL}^{-1}$) against *E. coli*, *P. aureginosa*, and *S. typhi*. The MIC value ($64\ \mu\text{g mL}^{-1}$) exhibited against *S. aureus* is different from these against all the other gram-positive bacteria.

The antibacterial applications of metal-organic frameworks have rarely been explained. Nomiya and co-workers presented the argument that polymeric Ag(I)-N bonding compounds had potential application in antibacterial materials against bacteria, yeast, and

Table 4. Antimicrobial activities of **1** as MIC values ($\mu\text{g mL}^{-1}$).

Micro-organisms	$[\text{Ag}_4(\mu\text{-pydc})_2(\mu\text{-pm})_2]_n$	AgNO_3	Vancomycin	Ciprofloxacin	Amphotericin-B
<i>Gram (\pm) bacteria</i>					
<i>MRSA</i>	256	32	1	0.5	–
<i>S. aureus</i>	64	16	1	0.25	–
<i>E. faecalis</i>	256	32	2	0.5	–
<i>B. cereus</i>	256	32	2	0.125	–
<i>L. monocytogenes</i>	256	16	2	0.5	–
<i>Gram (–) bacteria</i>					
<i>E. coli</i>	128	32	–	0.0625	–
<i>P. aureginosa</i>	128	32	–	0.0625	–
<i>S. typhi</i>	128	64	–	0.0625	–
<i>Yeast</i>					
<i>C. albicans</i>	4	<0.25	–	–	0.0625

mold [41]. Lu and co-workers reported bactericidal mechanism for $[\text{Ag}_5(\text{pydc})_2(\text{OH})]_n$, the release ability of Ag^+ ions and antibacterial activity of $[\text{Ag}_5(\text{pydc})_2(\text{OH})]_n$ toward *E. coli* and *S. aureus* [21].

As the first study of antimicrobial activity of mixed ligand silver-(pyridine-3,5-dicarboxylic acid) complex, **1** possesses good biological activity over the micro-organisms studied here. The antimicrobial behavior of **1** stems, presumably, from silver which may play an important role in antimicrobial activity since silver compounds are used as antimicrobial agents in many applications in medicine [41–45].

4. Conclusion

We have synthesized and characterized a 3-D silver(I) coordination polymer incorporating pyridine-3,5-dicarboxylate and pyrimidine. X-ray crystal structure analysis showed that **1** includes four crystallographically unique silver ions with different coordination environments and two different *pydc* ligands exhibiting different chelating and bridging modes. The magnitudes of intermetallic interactions playing important roles in the construction of 3-D crystal network have been revealed by NBO analysis in second-order energies and it is suggested that second-order interactions take place between high energy lone pair and Rydberg orbitals of Ag(I) centers, probably due to delocalizations of large 4d orbitals. The complex exhibits photoluminescence in the solid state at room temperature with two main emission peaks, maxima centered at 540 and 583 nm upon excitation at 386 nm. The luminescence intensity of **1** is much stronger than previously reported Ag(I) complexes with *pydc*, due to the direct metal–metal interactions and a larger HOMO–LUMO gap. Complex **1** showed broad antimicrobial activity against a series of bacterial and fungal agents. Especially, against the yeast *C. albicans*, antifungal activity of the complex was appreciable.

Supplementary material

CCDC 939295 contains the supplementary crystallographic data for $[\text{Ag}_4(\mu\text{-pydc})_2(\mu\text{-pm})_2]_n$. These data can be obtained free of charge via <http://www.ccdc.cam.ac.uk/contents/retrieving.html>, or from the Cambridge Crystallographic Data Center, 12 Union Road, Cambridge CB2 1EZ, UK; Fax: +44 1223 336 033; or E-mail: deposit@ccdc.cam.ac.uk.

Acknowledgements

The authors are grateful to the Research Fund of Ondokuz Mayıs University (Project No. PYO.MUH.1901.11.011) and Sinop University for financial support of this work. We also thank Assoc. Prof Okan Zafer Yeşilel for his assistance and Fatih Semerci in obtaining the luminescence spectra.

References

- [1] M. Eddaoudi, D.B. Moler, H. Li, B. Chen, T.M. Reinecke, M.O. Keeffe, O.M. Yaghi. *Acc. Chem. Res.*, **34**, 319 (2001).
- [2] G.S. Papaefstathiou, L.R. MacGillivray. *Coord. Chem. Rev.*, **246**, 169 (2003).
- [3] O.B. Moulton, M.J. Zaworotko. *Chem. Rev.*, **101**, 1629 (2001).
- [4] D. Farrusseng, S. Aguado, C. Pinel. *Angew. Chem., Int. Ed.*, **48**, 7502 (2009).
- [5] J.L.C. Rowsell, O.M. Yaghi. *Angew. Chem., Int. Ed.*, **44**, 4670 (2005).
- [6] S. Leininger, B. Olenyuk, P.J. Stang. *Chem. Rev.*, **100**, 853 (2000).
- [7] S. Zang, Y. Su, Y. Li, Z. Ni, Q. Meng. *Inorg. Chem.*, **45**, 174 (2006).
- [8] Z. Wang, S.M. Cohen. *Chem. Soc. Rev.*, **38**, 1315 (2009).
- [9] J.P. Zhang, X.C. Huang, X.M. Chen. *Chem. Soc. Rev.*, **38**, 2385 (2009).
- [10] O.Z. Yeşilel, G. Günay, C. Darcan, M.S. Soylu, S. Keskin, S.W. Ng. *Cryst. Eng. Commun.*, **14**, 2817 (2012).
- [11] E.J. Gao, X.F. Gu, Y.G. Sun, H.X. Yin, Q. Wu, L. Liu, M.C. Zhu, W.Z. Zhang. *Chin. J. Chem.*, **26**, 2133 (2008).
- [12] B.O. Patrick, C.L. Stevens, A. Storr, R.C. Thompson. *Polyhedron*, **24**, 2242 (2005).
- [13] Y. Wei, H. Hou, L. Li, Y. Fan, Y. Zhu. *Cryst. Growth Des.*, **5**, 1405 (2005).
- [14] C. Xie, Z. Zhang, X. Wang, X. Liu, G. Shen, R. Wang, D. Shen. *J. Coord. Chem.*, **57**, 1173 (2004).
- [15] H.L. Gao, L. Yi, B. Zhao, X.Q. Zhao, P. Cheng, D.Z. Liao, S.P. Yan. *Inorg. Chem.*, **45**, 5980 (2006).
- [16] L.J. Li, Y. Li. *J. Mol. Struct.*, **694**, 199 (2004).
- [17] G.X. Liu, H. Chen, K. Zhu, X.M. Ren. *J. Inorg. Organomet. Polym.*, **18**, 457 (2008).
- [18] J. Yao, W. Huang, H. Zhu, J. Fang, S. Gou. *Polyhedron*, **23**, 1169 (2004).
- [19] X. Feng, J.S. Zhao, L.Y. Wang, X.G. Shi. *Chinese, J. Struct. Chem.*, **29**, 290 (2010).
- [20] Y.H. Zhao, Z.M. Su, Y.M. Fu, K.Z. Shao, P. Li, Y. Wang, X.R. Hao, D.X. Zhu, S.D. Liu. *Polyhedron*, **27**, 583 (2008).
- [21] X. Lu, J. Ye, D. Zhang, R. Xie, R.F. Bogale, Y. Sun, L. Zhao, Q. Zhao, G. Ning. *J. Inorg. Biochem.*, **138**, 114 (2014).
- [22] Y.B. Xie, Q. Gao, C.Y. Zhang, J.H. Sun. *J. Solid State Chem.*, **182**, 1761 (2009).
- [23] C.C. Wang, P. Wang, G.S. Guo. *Trans. Met. Chem.*, **35**, 721 (2010).
- [24] G.M. Sheldrick. *Acta Crystallogr.*, **64**, 112 (2008).
- [25] A.L. Spek. *J. Appl. Cryst.*, **36**, 7 (2003).
- [26] A.L. Spek. *Acta Cryst.*, **D65**, 148 (2009).
- [27] Clinical and Laboratory Standards Institute (CLSI). *Methods of Dilution Antimicrobial Susceptibility Tests for Bacteria that Grow Aerobically, Approved Standard*, 7th Edn, pp. M7–A7, CLSI, Wayne, (2006).
- [28] National Committee for Clinical Laboratory Standards. *Reference method for broth dilution antifungal susceptibility testing of yeasts. Approved standard*, 2nd Edn, p M27–A2, NCCLS, Wayne, (2002).
- [29] 09 Gaussian, A.1 Revision, M.J. Frisch, G.W. Trucks, H.B. Schlegel, G.E. Scuseria, M.A. Robb, J.R. Cheeseman, G. Scalmani, V. Barone, B. Mennucci, G.A. Petersson, H. Nakatsuji, M. Caricato, X. Li, H.P. Hratchian, A.F. Izmaylov, J. Bloino, G. Zheng, J.L. Sonnenberg, M. Hada, M. Ehara, K. Toyota, R. Fukuda, J. Hasegawa, M. Ishida, T. Nakajima, Y. Honda, O. Kitao, H. Nakai, T. Vreven, J.A. Montgomery, Jr., J.E. Peralta, F. Ogliaro, M. Bearpark, J.J. Heyd, E. Brothers, K.N. Kudin, V.N. Staroverov, R. Kobayashi, J. Normand, K. Raghavachari, A. Rendell, J.C. Burant, S.S. Iyengar, J. Tomasi, M. Cossi, N. Rega, J.M. Millam, M. Klene, J.E. Knox, J.B. Cross, V. Bakken, C. Adamo, J. Jaramillo, R. Gomperts, R.E. Stratmann, O. Yazyev, A.J. Austin, R. Cammi, C. Pomelli, J.W. Ochterski, R.L. Martin, K. Morokuma, V.G. Zakrzewski, G.A. Voth, P. Salvador, J.J. Dannenberg, S. Dapprich, A.D. Daniels, O. Farkas, J.B. Foresman, J.V. Ortiz, J. Cioslowski, D.J. Fox, *Gaussian*, Taylor and Francis, Inc., Wallingford, CT (2009).
- [30] K. Nakamoto. *Infrared and Raman Spectra of Inorganic and Coordination Compounds*, 5th Edn, Wiley, New York, NY (1997).
- [31] L. Yang, D.R. Powell, R.P. Houser. *Dalton Trans.*, 955 (2007). doi:10.1039/B617136B
- [32] A.N. Khlobystov, A.J. Blake, N.R. Champness, D.A. Lemenovskii, A.G. Majouga, N.V. Zyk, M. Schröder. *Coord. Chem. Rev.*, **222**, 155 (2001).
- [33] K. Akhbari, A. Morsali, S. Rafiei, M. Zeller. *J. Organomet. Chem.*, **693**, 257 (2008).

- [34] A.E. Reed, F. Weinhold. *J. Chem. Phys.*, **78**, 4066 (1983).
- [35] A.E. Reed, F. Weinhold. *J. Chem. Phys.*, **83**, 1736 (1983).
- [36] A.E. Reed, R.B. Weinstock, F. Weinhold. *J. Chem. Phys.*, **83**, 735 (1985).
- [37] A.E. Reed, L.A. Curtiss, F. Weinhold. *Chem. Rev.*, **88**, 899 (1988).
- [38] J.W. Shin, H.J. Cho, K.S. Min. *Inorg. Chem. Commun.*, **16**, 12 (2012).
- [39] S.L. Zheng, J.P. Zhang, X.M. Chen, Z.L. Huang, Z.Y. Lin, W.T. Wong. *Chem. Eur. J.*, **9**, 3888 (2003).
- [40] S.L. Zheng, J.P. Zhang, W.T. Wong, X.M. Chen. *J. Am. Chem. Soc.*, **125**, 6882 (2003).
- [41] K. Nomiya, K. Tsuda, T. Sudoh, M. Oda. *J. Inorg. Biochem.*, **68**, 39 (1997).
- [42] S.H. Alisir, B. Sariboga, Y. Topcu, S.Y. Yang. *J. Inorg. Organomet. Polym.*, **23**, 1061 (2013).
- [43] P. Kleyi, R.S. Walmsley, M.A. Fernandes, N. Torto, Z.R. Tshentu. *Polyhedron*, **41**, 25 (2012).
- [44] M. Rai, A. Yadav, A. Gade. *Biotechnol. Adv.*, **27**, 76 (2009).
- [45] B.S. Atiyeh, M. Costigliola, S.N. Hayek, S.A. Dibo. *Burns*, **33**, 139 (2007).